Theoretical Study of Intramolecular S_N2 Reactions of 3-Halogen or 3-Hydroxypropanamides To Obtain β-Lactams

Pablo Campomanes, M. Isabel Menéndez, and Tomás L. Sordo*

Departamento de Química Física y Analítica, Facultad de Química, Universidad de Oviedo, Julián Clavería, 8, 33006. Oviedo, Principado de Asturias, Spain

Received: June 14, 2004; In Final Form: September 27, 2004

A theoretical study of the intramolecular cyclization of a series of propanamides to yield β-lactams was performed at the B3LYP/6-31+G(d,p) and MP2/6-31+G(d,p)//B3LYP/6-31+G(d,p) levels. The effect of the Cl^- and OH^- leaving groups and of several substituents on N1 and on C4 was investigated. As expected, OH^- is a much worse leaving group than Cl^-, rendering an energy barrier about 2 times larger. An SO_3^- substituent on N1 diminishes the energy barrier by destabilizing the intermediate prior to the rate-determining TS, whereas OH and OCH_3 substituents do not produce an appreciable effect. According to the MP2 method, one and two methyl substituents on C4 increase the energy barrier of the process. The simultaneous presence of a sulfonate group on N1 and a methyl group on C4 render the corresponding combined effect, while combination of an OH on N1 and two methyl groups on C4 is not simply additive.

Introduction

The β-lactam ring plays an important role in organic and medicinal chemistry due to its versatility in organic synthesis and its presence in antimicrobial antibiotics.[1−5] Many methods have been developed for the synthesis of this four-member cycle. Some of the major single-bond-forming reactions leading to production of the β-lactam ring are those involving formation of the N1−C4 bond (see Scheme 1). In fact, this is the synthetic route selected by Nature for biosynthesis of azetidinone-containing antibiotics.[6]

Most of the methods for preparing the β-lactam ring through formation of the N1−C4 bond involve intramolecular displacement of a leaving group attached to C4 with appropriately activated nitrogen. The simplest way of achieving this process is through displacements of primary halogens by the amide nitrogen under basic conditions. These cyclizations have been performed with a variety of bases under various reaction conditions.[1,7,8−11] C4 leaving groups other than halogen have also been reported for this type of transformation.[11−13] In several cases, intramolecular cyclizations are not successful and the amide N needs to be activated by groups that attenuate its acidity. Oxygen-substituted hydroxamates[13−16] and amides sulfonated at the N atom[17−24] have been used for this purpose. The initial sulfonation of the amide nitrogen is a particularly useful process that renders monobactams, an important type of monocyclic β-lactams.

In the present work we theoretically study formation of the azetidinone ring through the S_N2 processes shown in Scheme 1. A base is required for the reaction to start. We consider the hydroxyl anion as a model of the base acting in all the reactions.

We will investigate the influence on the energy barrier of the leaving group, of $-SO_3^-$ and −OR substituents on the amide nitrogen, and of introducing one or two methyl groups at C4. We will discuss the availability of this synthetic method, which is useful for the preparation of monobactams, precursors of sulfactams and 2-azetidinones disubstituted at C4.

SCHEME 1

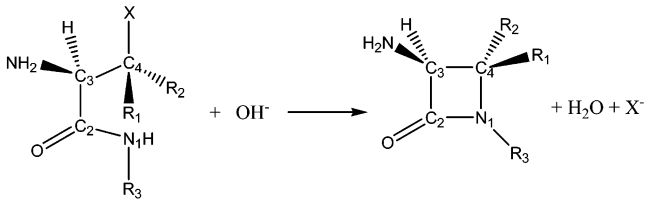

1 X = Cl $R_1 = R_2 = R_3 = H$
2 X = OH $R_1 = R_2 = R_3 = H$
3 X = Cl $R_1 = R_2 = H$, $R_3 = SO_3^-$
4 X = Cl $R_1 = R_2 = H$, $R_3 = OMe$
5 X = Cl $R_1 = R_2 = H$, $R_3 = OH$
6 X = Cl $R_1 = Me$, $R_2 = R_3 = H$
7 X = Cl $R_1 = R_2 = Me$, $R_3 = H$
8 X = Cl $R_1 = Me$, $R_2 = H$, $R_3 = SO_3^-$
9 X = Cl $R_1 = R_2 = Me$, $R_3 = OH$

Methods

Full optimizations at the B3LYP/6-31+G(d,p) level[25−32] were performed using the Gaussian98 series of programs.[33] The nature of the stationary points was further checked, and zero-point vibrational energies (ZPVE) were evaluated by analytical computations of harmonic vibrational frequencies at the same theory level. IRC calculations at the same level were also carried out to check the two minimum energy structures connected by each transition state (TS) using the Gonzalez and Schlegel method[34] implemented in Gaussian 98. Single-point MP2/6-31+G(d,p)//B3LYP/6-31+G(d,p) calculations were also performed to assess the accuracy of the B3LYP energies.[35]

ΔH, ΔS, and ΔG values were calculated within the ideal gas, rigid rotor, and harmonic oscillator approximations.[36] A pressure

* To whom correspondence should be addressed. E-mail: tsordo@uniovi.es

10.1021/jp047429n CCC: $27.50
Published on Web 11/16/2004

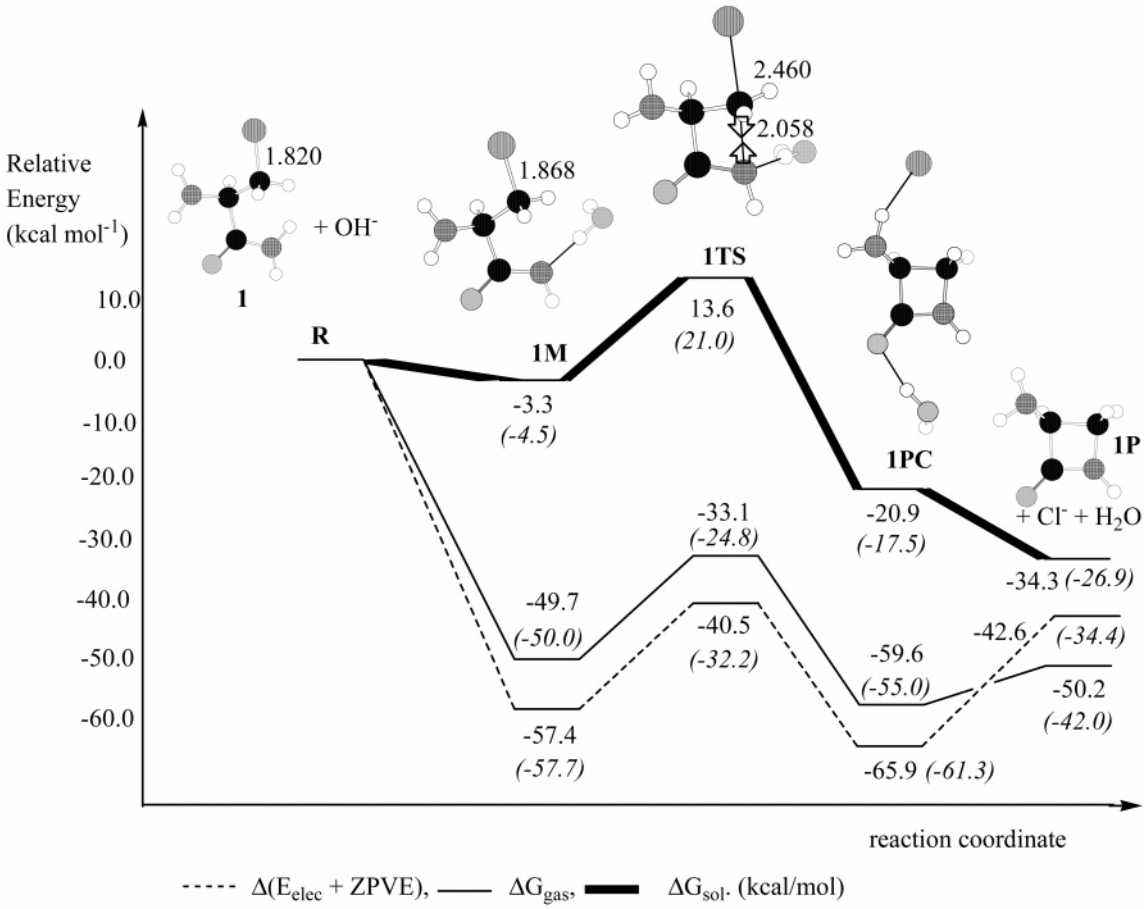

Figure 1. Energy profiles for reaction of 2-amino-3-chloropropanamide (**1**). B3LYP/6-31+G(d,p) values in plain figures and MP2/6-31+G(d,p)// B3LYP/6-31+G(d,p) in italic figures in parentheses. The most important components of the transition vector for **1TS** are depicted.

of 1 atm and a temperature of 298.15 K were assumed in the calculations.

Quantum chemical computations in solution were carried out on gas-phase-optimized geometries using a general self-consistent-reaction field (SCRF) model.[37−41] In this model the solvent is represented by a dielectric continuum characterized by its relative static dielectric permittivity, ϵ. The solute is placed in a cavity created in the continuum, the shape of which is chosen to fit as best as possible the solute molecular shape according to the solvent-accessible surface. The UAHF (united atom Hartree−Fock) parametrization[38] of the polarizable continuum model (PCM)[42−46] was used. Addition to ΔG_{gas} of the solvation Gibbs energy, $\Delta\Delta G_{solvation}$, gives $\Delta G_{solution}$. A relative permittivity of 7.58 was used to simulate THF as solvent.

An NBO population analysis[47] was performed using the version implemented in the Gaussian98 series of programs.

Results and Discussion

We present first the reaction of 2-amino-3-chloropropanamide (**1**) that can be considered as a reference for the remaining processes. Then the effect of the leaving group and the effects of substituents on the amide nitrogen and on C4 will be discussed.

Reaction of 2-Amino-3-chloropropanamide. Figure 1 displays the relative electronic energy (including ZPVE correction) and the relative Gibbs free energy in the gas phase and in THF solution obtained with B3LYP and MP2 methods for the reaction of 2-amino-3-chloropropanamide, **1**. Table 1S of the Supporting Information collects the corresponding absolute electronic energy, ZPVE, ΔH, $T\Delta S$, and $\Delta G_{solvation}$.

According to the B3LYP/6-31+G(d,p) calculations, the first stable structure along the electronic energy profile is the intermediate **1M** in which a proton has been transferred from the amide to the OH^- base. Due to the greater proton affinity of OH^- and the ability of $CH_2Cl-CHNH_2-CONH^-$ to stabilize by resonance, **1M** is as much as 57.4 kcal mol^{-1} more stable than separate reactants in electronic energy + ZPVE. The dihedral angle, C4−C3−C2−N1, reduces from −52.4° at the isolated amide to −35.1° at **1M** and the C4−chlorine bond starts to elongate (see Figure 1). Only one TS, **1TS**, was found for the reaction with an electronic energy barrier (including the ZPVE) of 16.9 kcal mol^{-1}. At **1TS** the dihedral angle C4−C3−C2−N1 is −11.0° and Cl^- anion is 2.460 Å away from C4, while N1 starts interacting with C4 at a distance of 2.058 Å. Pyramidalization at C4, measured by *w*, the summation of the three angles centered at C4, has almost disappeared (w = 359.7°) in its way to the final inversion. **1TS** connects **1M** with **1PC**, a complex prior to the product 65.9 kcal mol^{-1} more stable than separate reactants in which Cl^-, H_2O, and **1P** (3-amino-2-azetidinone) are interacting. The relative electronic energy including the ZPVE of the three isolated products, Cl^- + H_2O + **1P**, is −42.6 kcal mol^{-1}. We evaluated the effect of basis-set superposition error (BSSE) on the energy of **1M** and **1TS** by means of the Boys and Bernardi counterpoise correction.[48] When including the BSSE, both **1M** and **1TS** become 2.0 kcal mol^{-1} destabilized with respect to reactants, and consequently its effect on the energy barrier is null.

The thermal energy is practically the same for all critical structures along the reaction coordinate. Entropy destabilizes all the structures about 7−8 kcal mol^{-1} relative to separate

TABLE 1: Relative Electronic Energy Plus ZPVE, Relative Gibbs Energy in the Gas Phase, and Relative Gibbs Energy in THF Solution (all in kcal mol^{-1}) at B3LYP/6-31+G(d,p) and MP2/6-31+G(d,p)//B3LYP/6-31+G(d,p) Levels for the Critical Structures for the Reaction of 2. The Levels of the Calculations are Previously Displayed

	B3LYP/6-31+G(d,p)			MP2//B3LYP		
structures	Δ(E + ZPVE)	ΔG_{gas}	$\Delta G_{solution}$	Δ(E + ZPVE)	ΔG_{gas}	$\Delta G_{solution}$
reactants (**2** + OH^-)	0.0	0.0	0.0	0.0	0.0	0.0
2M	−51.1	−40.1	3.3	−52.4	−41.4	1.3
2TS	−5.3	2.2	42.6	−3.8	3.7	42.8
2PC	−23.7	−17.7	16.5	−23.2	−17.3	15.8
2P + H_2O + OH^-	13.7	4.9	3.5	14.6	5.9	4.2
barrier	45.8	42.3	42.6	48.6	44.8	42.8

reactants (see Table 1S), except for the separate products, which become stabilized by 8 kcal mol^{-1}. Consequently, in the gas phase the Gibbs energy barrier corresponding to **1TS** is 16.6 kcal mol^{-1} and the reaction is exothermic by 50.2 kcal mol^{-1} (see Figure 1). Both Δ(E + ZPVE) and ΔG_{gas} profiles proceed under reactants energy. At the MP2/6-31+G(d,p)//B3LYP/6-31+G(d,p) level the relative stability in electronic energy + ZPVE of **1M** is practically the same as with the B3LYP method, whereas **1TS** and the products become destabilized by about 8 kcal mol^{-1} and **1PC** by 4.6 kcal mol^{-1}, the Gibbs energy profile in gas phase paralleling this behavior.

THF solvent stabilizes all of the structures along the energy profile, but reactants are preferentially stabilized because of the negative charge in OH^-. As a consequence, in solution **1PC** becomes a transient structure, **1TS** is 13.6 (B3LYP), 21.0 (MP2) kcal mol^{-1} less stable than reactants, and the Gibbs energy barrier from **1M** amounts to 16.9 (B3LYP) and 25.5 (MP2) kcal mol^{-1}. In THF solution the reaction is exothermic by 34.3 (B3LYP) and 26.9 (MP2) kcal mol^{-1}.

Effect of the Leaving Group. For 2-amino-3-hydroxypropanamide, **2**, the reaction proceeds analogously through intermediate **2M**, TS **2TS**, and complex **2PC** to yield the 2-azetidinone product. Table 1 collects the relative electronic energy + ZPVE and the relative Gibbs energy in the gas phase and THF solution for the critical structures located along the reaction coordinate for 2-amino-3-hydroxypropanamide. Table 2S of the Supporting Information collects the corresponding absolute electronic energy, ZPVE, ΔH, $T\Delta S$, and $\Delta G_{solvation}$.

As expected, Table 1 shows that OH^- is a much worse leaving group than Cl^-. In effect, **2TS** has a later character than **1TS** (the N1−C4 distance is 1.881 Å in **2TS** and 2.058 Å in **1TS**, and the leaving OH^- and Cl^- present their bond to C4 stretched in 52% and 35%, respectively). **2TS** displays a much smaller relative stability with respect to reactants than **1TS** , so that the corresponding energy barrier is now 45.8 (B3LYP) and 48.6 (MP2) kcal mol^{-1} in electronic energy + ZPVE, and the process is endoergic by 13.7 (B3LYP) and 14.6 (MP2) kcal mol^{-1}. The thermal energy is very similar for all the critical structures. Entropy destabilizes **2M**, **2TS,** and **2PC** by 11.7, 7.9, and 5.9 kcal mol^{-1}, respectively, whereas it stabilizes the products by 9.5 kcal mol^{-1}. As a consequence, in the gas phase the Gibbs energy barrier for **2TS** is 42.3 (B3LYP) and 45.1 (MP2) kcal mol^{-1} and the endothermicity of the process is 4.9 (B3LYP) and 5.9 (MP2) kcal mol^{-1}.

The interaction with solvent preferentially stabilizes the reactants owing to the negative charge of the OH^- base transforming **2M** and **2PC** in transient species, giving rise to a concerted process with a barrier of 42.6 (B3LYP) and 42.8 (MP2) kcal mol^{-1} and an endothermicity of 3.5 (B3LYP) and 4.2 (MP2) kcal mol^{-1} in $\Delta G_{solution}$.

Effect of Substituents on the Amide Nitrogen. We considered three different substituents on the amide N: $-SO_3^-$, $-OCH_3$, and $-OH$. Figure 2 displays the relative electronic energy (including the ZPVE correction) and the relative Gibbs energy in the gas phase and THF solution for reaction of 2-amino-3-chloro-1-sulfonatepropanamide anion, **3**. Table 3S of the Supporting Information lists the corresponding absolute electronic energy, ZPVE, ΔH, $T\Delta S$, and $\Delta G_{solvation}$.

The B3LYP/6-31+G(d,p) proton affinity of the amide N in **3** in the gas phase is 31.4 kcal mol^{-1} greater than that of OH^-. Thus, proton transfer to yield **3M** is an endoergic process by 11.6 kcal mol^{-1} in electronic energy + ZPVE, with an energy barrier equal to this endoergicity because no TS was located for it (see Figure 2). The interacting water molecule in **3M** rearranges through a small barrier of 0.7 kcal mol^{-1} to a more stable conformation **3M′** in which it interacts with two oxygen atoms of the SO_3^- group. **3M′**evolves through the rate-limiting TS **3TS** 14.8 kcal mol^{-1} less stable than separate reactants to form a complex 25.2 kcal mol^{-1} less than reactants in which the products Cl^-, 3-amino-2-azetidine-1-sulfonate ion, and H_2O are interacting. This complex dissociates to yield the final products 42.8 kcal mol^{-1} more stable than reactants. It is interesting to note that **3TS** is an earlier TS than **1TS,** as clearly indicated by longer N1−C4 and shorter C4−Cl distances (see Figures 1 and 2). When including the BSSE, **3M′** and **3TS** become 2.9 and 2.7 kcal mol^{-1} destabilized with respect to reactants, respectively, and accordingly the corrected rate-determining energy barrier for reaction **3** would be 2.7 kcal mol^{-1} larger.

The thermal energy stabilizes **3M**, **3TS′**, **3M′**, and **3TS** with respect to reactants by about 1.5 kcal mol^{-1}, **3PC** by 0.8 kcal mol^{-1}, and products by only 0.3 kcal mol^{-1}. With respect to reactants, entropy destabilizes about 6−10 kcal mol^{-1} all the structures except for the products, which become about 8 kcal mol^{-1} stabilized. Consequently, in the gas phase the Gibbs energy barrier corresponding to **3TS** is 23.5 kcal mol^{-1} and the exothermicity of the process is 50.5 kcal mol^{-1}.

At the MP2/6-31+G(d,p)//B3LYP/6-31+G(d,p) level the electronic energy + ZPVE profile is quite similar to the B3LYP one up to **3M′** whereas **3TS**, **3PC,** and the products become destabilized with respect to the B3LYP results by 7.3, 3.5, and 6.1 kcal mol^{-1}, respectively, the **3TS** Gibbs energy barrier and the exothermicity of the process in the gas-phase being 30.9 and 44.4 kcal mol^{-1}.

Interaction with solvent now stabilizes **3M**, **3TS′**, **3M′**, and **3TS** with respect to reactants by about 9−18 kcal mol^{-1}, whereas **3PC** and the products become disfavored by about 2−3 and 13−14 kcal mol^{-1}, respectively. As a consequence, in solution the Gibbs energy barrier for the process amounts to 14.2 (B3LYP) and 21.0 (MP2) kcal mol^{-1}. This barrier is 2.7 (B3LYP) and 4.5 (MP2) kcal mol^{-1} lower than that for reactant **1** because proton transfer to the OH^- base is endothermic, rendering less stable intermediates **3M** and **3M′** compared to **1M**. In solution the exothermicity of the process is 37.3 (B3LYP) and 31.6 (MP2) kcal mol^{-1}.

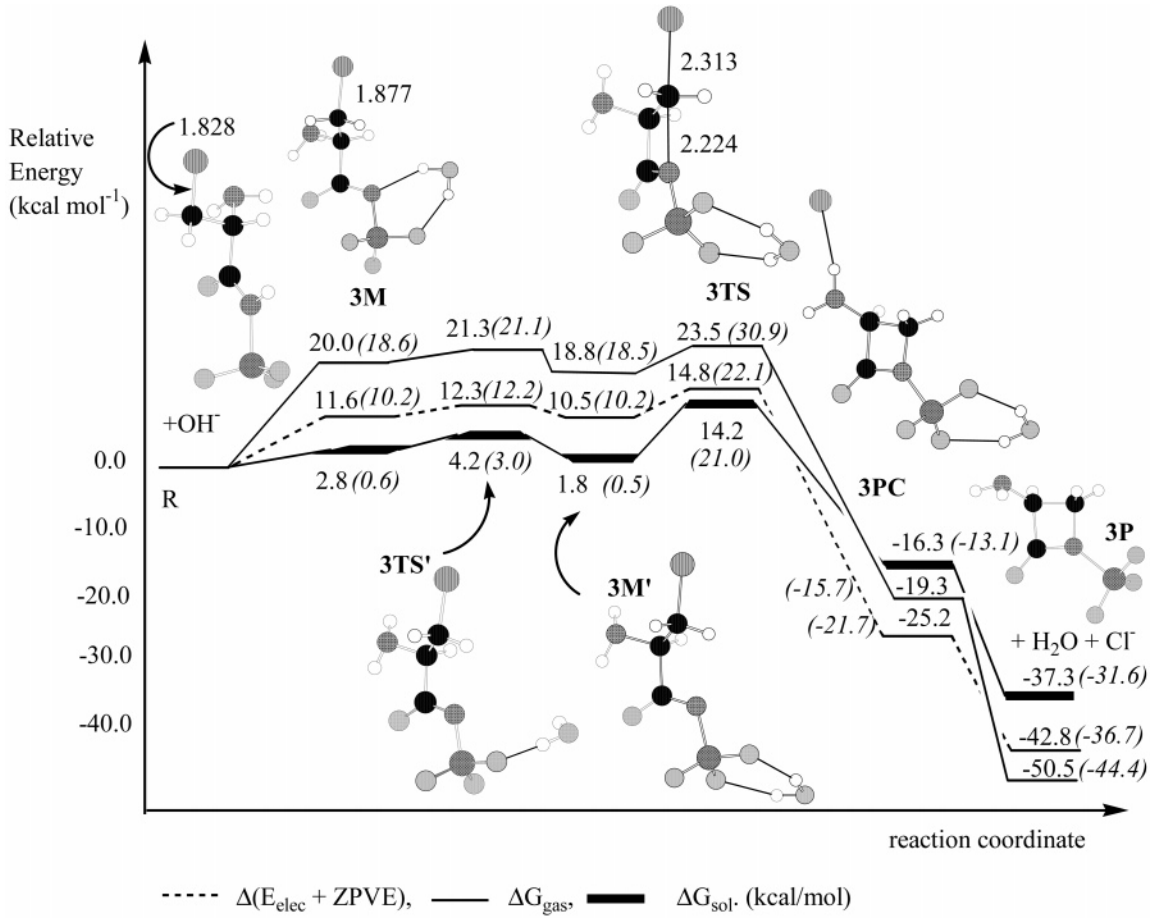

Figure 2. Energy profiles for the reaction of 2-amino-3-chloro-1-sulfonatepropanamide (**3**). B3LYP/6-31+G(d,p) values in plain figures and MP2/6-31+G(d,p)//B3LYP/6-31+G(d,p) in italic figures in parentheses.

TABLE 2: Relative Electronic Energy Plus ZPVE, Relative Gibbs Energy in the Gas Phase, and Relative Gibbs Energy in THF Solution (all in kcal mol^{-1}) at B3LYP/6-31+G(d,p) and MP2/6-31+G(d,p)//B3LYP/6-31+G(d,p) Levels for the Critical Structures for the Reactions of 4 and 5

	B3LYP/6-31+G(d,p)			MP2//B3LYP		
structures	Δ(E + ZPVE)	ΔG_{gas}	$\Delta G_{solution}$	Δ(E + ZPVE)	ΔG_{gas}	$\Delta G_{solution}$
reactants (**4** + OH^-)	0.0	0.0	0.0	0.0	0.0	0.0
4M	−65.7	−58.7	−10.7	−67.8	−60.8	−13.9
4TS	−49.1	−41.7	6.7	−42.6	−35.2	12.6
4PC	−67.7	−62.2	−20.6	−66.1	−60.6	−19.8
4P + H_2O + OH^-	−47.7	−55.8	−39.7	−39.7	−47.8	−32.1
barrier	16.6	17.0	17.4	25.2	25.6	26.5
reactants (**5** + OH^-)	0.0	0.0	0.0	0.0	0.0	0.0
5M	−63.7	−56.7	−10.2	−65.1	−58.1	−13.3
5TS	−47.7	−40.0	6.8	−40.3	−32.6	13.3
5PC	−67.6	−61.0	−22.4	−65.6	−59.0	−21.0
5P + H_2O + OH^-	−45.7	−53.5	−37.7	−38.5	−46.4	−31.9
barrier	16.0	16.7	17.0	24.8	25.5	26.6

When the substituent on the amide N is −OR (R = CH_3, 2-amino-3-chloro-1-methoxypropanamide, **4**; R = H, 2-amino-3-chloro-1-hydroxypropanamide, **5**) the mechanism of the process and the corresponding energy profile are analogous to those for reactant **1** above. Table 2 collects the relative electronic energies + ZPVE and the relative Gibbs energies in the gas phase and THF solution. Table 4S of the Supporting Information lists the corresponding absolute electronic energies, ZPVE, ΔH, $T\Delta S$, and $\Delta G_{solvation}$.

In solution both the minima **4M** and **5M** and the limiting TSs, **4TS** and **5TS**, are more stable than **1M** and **1TS** by practically the same amount (about 7 (B3LYP) and 8−9 (MP2) kcal mol^{-1}), rendering energy barriers for **4TS** of 17.4 (B3LYP) and 26.5 (MP2) kcal mol^{-1} and for **5TS** of 17.0 (B3LYP) and 26.6 (MP2) kcal mol^{-1}, similar to that for reactant **1**. These two processes are more exothermic than the reaction of **1** with Gibbs energies of reaction in solution of 39.7 (B3LYP) and 32.1 (MP2) kcal mol^{-1} for the reaction of **4** and 37.7 (B3LYP) and 31.9 (MP2) kcal mol^{-1} for the reaction of **5**.

Effect of Substituents on C4. We investigated the effect of one (reactant **6**) and two (reactant **7**) methyl substituents on C4.

The 2-amino-3-chloro-3-methylpropanamide has two isomer forms depending on the configuration at C4 (*S* or *R*): **6S** and **6R**. In the three reactions of **6S**, **6R**, and **7** the reaction mechanism and the energy profiles are qualitatively similar to those for reactant **1**. Table 3 presents the relative electronic energies + ZPVE and the relative Gibbs energies in the gas

TABLE 3: Relative Electronic Energy Plus ZPVE, Relative Gibbs Energy in the Gas Phase, and Relative Gibbs Energy in THF Solution (all in kcal mol^{-1}) at B3LYP/6-31+G(d,p) and MP2/6-31+G(d,p)//B3LYP/6-31+G(d,p) Levels for the Critical Structures for the Reactions of 6 and 7

	B3LYP/6-31+G(d,p)			MP2//B3LYP		
structures	Δ(E + ZPVE)	ΔG_{gas}	$\Delta G_{solution}$	Δ(E + ZPVE)	ΔG_{gas}	$\Delta G_{solution}$
reactants (**6S** + OH^-)	0.0	0.0	0.0	0.0	0.0	0.0
6SM	−57.1	−49.5	−2.6	−57.5	−50.0	−3.9
6STS	−39.5	−32.4	15.8	−29.4	−22.3	24.9
6SPC	−67.2	−60.7	−21.3	−62.0	−55.5	−17.5
6SP + H_2O + OH^-	−43.5	−51.6	−35.6	−34.2	−42.2	−27.0
barrier	17.6	17.1	18.4	28.1	27.7	28.8
reactants (**6R** + OH^-)	0.0	0.0	0.0	0.0	0.0	0.0
6RM	−56.0	−49.0	−1.9	−56.8	−49.8	−3.5
6RTS	−38.1	−30.9	17.7	−27.0	−19.8	27.5
6RPC	−69.0	−62.5	−21.7	−57.0	−50.5	−10.6
6RP + H_2O + OH^-	−44.7	−52.7	−36.2	−35.0	−43.0	−27.3
barrier	17.9	18.1	19.6	29.8	30.0	31.0
reactants (**7** + OH^-)	0.0	0.0	0.0	0.0	0.0	0.0
7M	−55.9	−48.8	−1.3	−56.7	−49.6	−2.6
7TS	−41.3	−34.9	13.1	−26.3	−19.8	27.3
7PC	−71.2	−64.9	−22.8	−65.4	−59.1	−18.1
7P + H_2O + OH^-	−46.6	−55.2	−38.7	−35.9	−44.5	−28.4
barrier	14.6	13.9	14.4	30.4	29.8	29.9

TABLE 4: Relative Electronic Energy Plus ZPVE, Relative Gibbs Energy in the Gas Phase, and Relative Gibbs Energy in THF Solution (all in kcal mol^{-1}) at B3LYP/6-31+G(d,p) and MP2/6-31+G(d,p)//B3LYP/6-31+G(d,p) Levels for the Critical Structures for the Reactions of 8 and 9

	B3LYP/6-31+G(d,p)			MP2//B3LYP		
structures	Δ(E + ZPVE)	ΔG_{gas}	$\Delta G_{solution}$	Δ(E + ZPVE)	ΔG_{gas}	$\Delta G_{solution}$
reactants (**8S** + OH^-)	0.0	0.0	0.0	0.0	0.0	0.0
8SM	10.8	19.2	3.9	9.0	17.4	1.2
8STS′	11.7	20.3	4.5	11.3	19.9	3.2
8SM′	9.8	17.9	2.7	9.2	17.3	0.8
8STS	14.8	22.6	14.7	24.2	32.0	23.1
8SPC	−26.4	−20.1	−16.2	−23.0	−16.7	−13.3
8SP + H_2O + OH^-	−43.6	−51.6	−38.1	−37.4	−45.3	−32.2
barrier	14.8	22.6	14.7	24.2	32.0	23.1
reactants (**8R** + OH^-)	0.0	0.0	0.0	0.0	0.0	0.0
8RM	11.4	19.7	4.0	9.7	17.9	1.4
8RTS′	13.1	21.7	3.7	12.5	21.1	1.8
8RM′	11.7	20.1	5.2	12.9	21.2	4.9
8RTS	15.7	23.8	15.9	25.9	34.0	24.7
8RPC	−27.2	−21.3	−17.5	−23.0	−17.0	−14.5
8RP+ H_2O + OH^-	−45.5	−53.2	−39.4	−38.5	−46.2	−33.2
barrier	15.7	23.8	15.9	25.9	34.0	24.7
reactants (**9** + OH^-)	0.0	0.0	0.0	0.0	0.0	0.0
9M	−54.6	−47.2	−1.8	−55.8	−48.4	−3.8
9TS	−43.6	−37.3	8.7	−30.3	−23.9	20.8
9PC	−74.2	−67.0	−26.0	−70.0	−62.8	−22.8
9P + H_2O + OH^-	−45.6	−53.9	−39.7	−37.1	−45.5	−31.8
barrier	11.0	9.9	10.5	25.5	24.5	24.6

phase and THF solution. Table 5S of the Supporting Information lists the corresponding absolute electronic energies, ZPVE, ΔH, $T\Delta S$, and $\Delta G_{solvation}$.

For the reactions of **6S** and **6R** we obtained a Gibbs energy barrier in solution of 18.4 (B3LYP) and 28.8 (MP2) kcal mol^{-1} and 19.6 (B3LYP) and 31.0 (MP2) kcal mol^{-1}, respectively, and the exothermicity of the processes is 35.6 (B3LYP) and 27.0 (MP2) kcal mol^{-1} and 36.2 (B3LYP) and 27.3 (MP2) kcal mol^{-1}. These energy barriers are higher than that for the reaction of **1**. For the reaction of **7** in solution the B3LYP method yields a Gibbs energy barrier of 14.4 kcal mol^{-1}, 2.5 kcal mol^{-1} lower than that for **1**, and an exothermicity of 38.7 kcal mol^{-1}, whereas the MP2 method renders a Gibbs energy barrier of 29.9 kcal mol^{-1}, 4.4 kcal mol^{-1} higher than that for **1**, and the process is exothermic by 28.4 kcal mol^{-1}. It is interesting to note that at the TSs for the reactions of **6S** and **6R** (**6STS** and **6RTS**) the distances N1−C4 (2.158 and 2.180 Å) and C4−Cl (2.602 and 2.613 Å) are slightly longer than those in **1TS** (see Figure 1), whereas in **7TS** both distances (N1−C4 = 2.523 Å; C4−Cl = 3.166 Å) are significantly more stretched than in **1TS**. Therefore, **6STS** and **6RTS** present an earlier character than **1TS** with respect to N1−C4 bond formation but a later character with respect to Cl^- elimination. This earlier and later character is still more pronounced in **7TS**.

Simultaneous Methyl Substitution on C4 and OR Substitution on N1. We studied the reaction of the two isomers of 2-amino-3-chloro-3-methyl-1-sulfonatepropanamide anion, **8S** and **8R**, and 2-amino-3,3-dimethyl-1-hydroxypropanamide, **9**. Table 4 collects the electronic energy + ZPVE and the relative Gibbs energy in the gas phase and THF solution of the critical structures located along the three reaction coordinates. Table 6S in the Supporting Information lists the corresponding absolute electronic energies, ZPVE, ΔH, $T\Delta S$, and $\Delta G_{solvation}$.

For the reaction of **8S** and **8R** we obtained energy profiles qualitatively similar to those for reactant **3**. In **8STS** and **8RTS** the C4−Cl bond distances are similar (2.472 and 2.446 Å,

respectively) to that in **1TS** whereas the N1−C4 distances are larger (2.293 and 2.327 Å), indicating that these TSs are earlier than **1TS** with respect to ring formation. The Gibbs energy barriers in solution corresponding to **8STS** and **8RTS** are, respectively, 14.7 (B3LYP) and 23.1 (MP2) kcal mol^{-1} and 15.9 (B3LYP) and 24.7 (MP2) kcal mol^{-1}. These energy barriers are between those for reactants **3** and **6**. The reactions of **8S** and **8R** are exothermic processes by 38.1 (B3LYP) and 32.2 (MP2) kcal mol^{-1} and 39.4 (B3LYP) and 33.2 (MP2) kcal mol^{-1}, respectively.

For **9** the energy profiles are analogous to that for **1**. In **9TS** both N1−C4 (2.457 Å) and C4−Cl (2.948 Å) distances are longer than those in **1TS**. The Gibbs energy barrier in solution is 10.5 (B3LYP) and 24.6 (MP2) kcal mol^{-1}, and the exothermicity is 39.7 (B3LYP) and 31.8 (MP2) kcal mol^{-1}. The energy barrier is now 6.4 (B3LYP) and 0.9 (MP2) kcal mol^{-1} lower than that for **1**.

Discussion

We discuss now the general trends observed in Gibbs energy profiles in solution owing to the effects of the different substituents considered in the present study. The rate-determining TS, **3TS**, presents an earlier character than **1TS**, and the presence of a SO_3^- substituent on the amide nitrogen atom diminishes the energy barrier because the minimum energy structure prior to **3TS** becomes destabilized with respect to reactants. This is a consequence of the difficulty of the proton transfer from the anion reactant to the OH^- base producing a dianionic species. The OR groups (R = H, Me) on the amide nitrogen atom give rise to a more stable energy profile determining approximately the same energy barrier and similar N1−C4 and C4−Cl distances than in **1TS**.

According to MP2 results one methyl group and two methyl groups on C4 both render a higher energy barrier. In contrast, with the B3LYP method two methyl groups on C4 destabilize mainly the minimum energy structure prior to the rate-determining TS, producing a lower energy barrier. To understand the effect produced by one or two methyl groups on C4 on the nature of the TSs, we take into account that C4 acts in these S_N2 processes both as an electron acceptor (from N1) and as an electron donor (to Cl). From the MP2 NBO charge of C4, Q, we see that in **6S** ($Q = -0.23$ e) and **6R** ($Q = -0.25$ e) C4 is a better electron acceptor (worse donor) than in **1** ($Q = -0.43$ e), and consequently, **6STS** and **6RTS** present an earlier character than **1TS** with respect to the cyclization and a later character with respect to Cl^- elimination. In **7** ($Q = -0.05$ e) C4 is even a much better electron acceptor (worse donor) than in **6S** and **6R,** so that the earlier and later character of **6STS** and **6RTS** is even more enhanced in **7TS**.

8STS and **8RTS** display the effect of SO_3^- substitution on N1 and a methyl group on C4, and therefore, they are earlier than **6STS**, **6RTS,** and **3TS** with respect to N1−C4 closure but have a similar degree of Cl^- elimination to **1TS**. By assuming that an earlier character of the TS implies a lower energy barrier and a later character a larger energy barrier, we can understand that the corresponding energy barriers for **8S** and **8R** are between those for **3** and **6S**/**6R**.

The combined effects of −OH on N1 and the two methyl groups on C4 render a TS **9TS** more stable relative to reactants and a lower Gibbs energy barrier in solution relative to previous intermediate than in the case of **1TS**. This indicates that the effect of these substituents is not simply additive.

As OH^- is a worse leaving group than Cl^-, **2TS** is significantly later in character than **1TS** and has a considerably larger Gibbs energy barrier in solution.

Acknowledgment. We thank the Principado de Asturias for financial support (PB02-045).

Supporting Information Available: Absolute electronic energies, ZPVE corrections, relative enthalpies, relative entropies, Gibbs energies of solvation in THF, and Cartesian coordinates for all critical structures for the reactions studied in this paper. This material is available free of charge via the Internet at http://pubs.acs.org.

References and Notes

(1) Commercon, A.; Ponsinet, G. *Tetrahedron Lett.* **1983**, *24*, 3725.
(2) Southgate, R. *Contemp. Org. Synth.* **1994**, *1*, 417.
(3) Page, M. I. *The Chemistry of beta-lactams*; Blackie Academic & Professional: London, 1992; Vol. 43.
(4) Nicolaou, K. C.; Sorensen, E. J. *Classics in Total Synthesis*; VCH: Weinheim, 1996.
(5) Georg, G. I. *The Organic Chemistry of beta-lactams*; VCH: Weinheim, 1992.
(6) Queener, S. W.; Neuss, N. In *Chemistry and Biology of beta-lactam antibiotics*; Morin, R. B., Gorman, M., Eds.; Academic Press: New York, 1982; Vol. 3, p 1.
(7) Takahata, H.; Ohnishi, Y.; Yamazaki, T. *Heterocycles* **1980**, *14*, 467.
(8) Abdulla, R. F.; Williams, J. C., Jr *Tetrahedron Lett.* **1980**, *21*, 997.
(9) Sebati, S.; Foucaud, A. *Tetrahedron* **1984**, *40*, 3223.
(10) Floyd, D. M.; Fritz, A. W.; Plusec, J.; Weaver, E. R.; Cimarusti, C. M. *J. Org. Chem.* **1982**, *47*, 5160.
(11) Song, C. E.; Lee, S. W.; Roh, E. J.; Lee, S. G.; Lee, W. K. *Tetrahedron: Asymmetry* **1998**, *9*, 983.
(12) Adlington, R. M.; Barret, A. G. M.; Quayle, P.; Walker, A. *J. Chem. Soc., Chem. Commun.* **1981**, 404.
(13) Miyata, O.; Fujiwara, Y.; Ninomiya, I.; Naito, T. *J. Chem. Soc., Perkin Trans. 1* **1998**, *14*, 2167.
(14) Rajendra, G.; Miller, M. J. *Tetrahedron Lett.* **1985**, *26*, 5385.
(15) Rajendra, G. M. *Tetrahedron Lett.* **1987**, *28*, 6257.
(16) Rajendra, G. M. *J. Org. Chem.* **1987**, *52*, 4471.
(17) Floyd, D. M.; Fritz, A. W.; Cimarusti, C. M. *J. Org. Chem.* **1982**, *47*, 176.
(18) Floyd, D. M.; Fritz, A. W.; Cimarusti, C. M. *J. Org. Chem.* **1982**, *47*, 179.
(19) Cimarusti, C. M.; Bonner, D. P.; Breuer, H.; Chang, H. W.; Fritz, A. W.; Floyd, D. M.; Kissick, T. P.; Koster, W. H.; Kronenthal, D.; Massa, F.; Mueller, R. H.; Pluscec, J.; Slusarchyck, W. A.; Sykes, R. T. B.; Taylor, M.; Weaver, E. R. *Tetrahedron* **1983**, *39*, 2577.
(20) Cardani, S.; Bernardi, A.; Colombo, L.; Scolastico, C.; Venturini, I.; Gennari, C. *Tetrahedron* **1988**, *44*, 5563.
(21) Herranz, R.; Conde, S.; Fernández-Resa, P.; Arribas, E. *J. Chem. Soc., Perkin Trans. 1* **1988**, 649.
(22) Wei, C. C.; Debernardo, S.; Tengi, J. P.; Borgese, J.; Weigele, M. *J. Org. Chem.* **1985**, *50*, 3462.
(23) Manchand, P. S.; Luk, K. C.; Belica, P. S.; Choudhry, S. C.; Wei, C. C.; Soukup, M. *J. Org. Chem.* **1988**, *53*, 5507.
(24) Jackson, B. G.; Pedersen, S. W.; Fisher, J. W.; Misner, J. W.; Gardner, J. P.; Staszak, M. A.; Doecke, C.; Rizzo, J.; Aikins, J.; Farkas, E.; Trinkle, K. L.; Vicenzi, J.; Reinhard, M.; Kroeff, E. P.; Higginbotham, C. A.; Gazak, R. J.; Zhang, T. Y. *Tetrahedron* **2000**, *56*, 5667.
(25) Becke, A. D. *Phys. Rev. A* **1988**, *38*, 3098.
(26) Lee, C. Y., W.; Parr, R. G. *Phys. Rev. B* **1988**, *37*, 785.
(27) Becke, A. D. *J. Chem. Phys* **1993**, *98*, 5648.
(28) Watchers, A. J. H. *J. Chem. Phys.* **1970**, *52*, 1033.
(29) Hay, P. J. *J. Chem. Phys.* **1977**, *66*, 4377.
(30) Raghavachari, K. T.; G. W. *J. Chem. Phys.* **1989**, *91*, 1062.
(31) McLean, A. D. C.; G. S. *J. Chem. Phys.* **1980**, *72*, 5639.
(32) Krishnan, R. B.; J. S.; Seeger, R.; Pople, J. A. *J. Chem. Phys.* **1980**, *72*, 650.
(33) Frisch, M. J.; Trucks, G. W.; Schlegel, H. B.; Scuseria, G. E.; Robb, M. A.; Cheeseman, J. R.; Zakrzewski, V. G.; Montgomery, J. A., Jr.; Stratmann, R. E.; Burant, J. C.; Dapprich, S.; Millam, J. M.; Daniels, A. D.; Kudin, K. N.; Strain, M. C.; Farkas, O.; Tomasi, J.; Barone, V.; Cossi, M.; Cammi, R.; Mennucci, B.; Pomelli, C.; Adamo, C.; Clifford, S.; Ochterski, J.; Petersson, G. A.; Ayala, P. Y.; Cui, Q.; Morokuma, K.; Malick, D. K.; Rabuck, A. D.; Raghavachari, K.; Foresman, J. B.; Cioslowski, J.; Ortiz, J. V.; Stefanov, B. B.; Liu, G.; Liashenko, A.; Piskorz, P.; Komaromi, I.; Gomperts, R.; Martin, R. L.; Fox, D. J.; Keith, T.; Al-Laham, M. A.; Peng, C. Y.; Nanayakkara, A.; Gonzalez, C.; Challacombe, M.; Gill, P. M.

W.; Johnson, B.; Chen, W.; Wong, M. W.; Andres, J. L.; Gonzalez, C.; Head-Gordon, M.; Replogle, E. S.; Pople, J. A. *Gaussian98*; Gaussian, Inc.: Pittsburgh, PA, 1998.

(34) Schlegel, H. B. *J. Comput. Chem.* **1982**, *3*, 214.

(35) Hehre, W. J.; Radom, L.; Pople, J. A.; Schleyer, P. v. R. *Ab initio Molecular Orbital Theory*; John Wiley and Sons Inc.: New York, 1986.

(36) McQuarrie, D. A. *Statistical Mechanics*; Harper & Row: New York, 1976.

(37) Rivail, J. L.; R., D.; Ruiz-López, M. F. In *NATO ASI Series C*; Formosinho, S. J., Csizmadia, I. G., Arnaut, L., Eds.; Kluwer Academic Publishers: Dordrecht, 1991; Vol. 339, p 79.

(38) Tomasi, J. P., M. *Chem. Rev.* **1994**, *94*, 2027.

(39) Cramer, C. J. T.; D. G. In *Reviews in Computational Chemistry*; Lipkowitz, K. B. B., D. B., Eds.; VCH: New York, 1995; Vol. 6, pp 1−81.

(40) Rivail, J. L. R., D. In *Computational Chemistry: Review of Current Trends*; Leszczynski, J., Ed.; World Scientific: New York, 1995; pp 139−174.

(41) Cramer, C. J. T.; D. G. In *Chem. Rev.* **1999**, *99*, p 2161.

(42) Miertus, S. S., E.; Tomasi, J. *Chem. Phys.* **1981**, *55*, 117.

(43) Cammi, R. T., J. *J. Comput. Chem.* **1995**, *16*, 1449.

(44) Cossi, M. B., V.; Cammi, R.; Tomasi, J. *Chem. Phys. Lett.* **1996**, *255*, 327.

(45) Barone, V. C., M.; Tomasi, J. *J. Chem. Phys.* **1997**, *107*, 3210.

(46) Amovilli, C. B., V.; Cammi, R.; Cancès, E.; Cossi, M.; Menucci, B.; Pomelli, C. S.; Tomasi, J. *Adv. Quantum Chem.* **1998**, *32*, 227.

(47) Reed, A. E.; Curtiss, L. A.; Weinhold, R. *Chem. Rev.* **1988**, *88*, 899.

(48) Boys, S. F. B., F *Mol. Phys.* **1970**, *19*, 553.